De Novo Discovery of High-Affinity Peptide Binders for the SARS-CoV-2 Spike Protein

Citation: Pomplun, Sebastian et al. "De Novo Discovery of High-Affinity Peptide Binders for the SARS-CoV-2 Spike Protein." ACS Central Science 7, 1 (December 2020): 156–163 © 2020 American Chemical Society

As Published: http://dx.doi.org/10.1021/acscentsci.0c01309

Publisher: American Chemical Society (ACS)

Persistent URL: https://hdl.handle.net/1721.1/129679

Version: Final published version: final published article, as it appeared in a journal, conference proceedings, or other formally published context

ACS central science

http://pubs.acs.org/journal/acscii

Research Article

De Novo Discovery of High-Affinity Peptide Binders for the SARS-CoV-2 Spike Protein

Sebastian Pomplun, Muhammad Jbara, Anthony J. Quartararo, Genwei Zhang, Joseph S. Brown, Yen-Chun Lee, Xiyun Ye, Stephanie Hanna, and Bradley L. Pentelute*

Cite This: *ACS Cent. Sci.* 2021, 7, 156−163

Read Online

ACCESS | Metrics & More | Article Recommendations | Supporting Information

ABSTRACT: The β-coronavirus SARS-CoV-2 has caused a global pandemic. Affinity reagents targeting the SARS-CoV-2 spike protein are of interest for the development of therapeutics and diagnostics. We used affinity selection−mass spectrometry for the rapid discovery of synthetic high-affinity peptide binders for the receptor binding domain (RBD) of the SARS-CoV-2 spike protein. From library screening with 800 million synthetic peptides, we identified three sequences with nanomolar affinities (dissociation constants K_d = 80−970 nM) for RBD and selectivity over human serum proteins. Nanomolar RBD concentrations in a biological matrix could be detected using the biotinylated lead peptide in ELISA format. These peptides do not compete for ACE2 binding, and their site of interaction on the SARS-CoV-2-spike-RBD might be unrelated to the ACE2 binding site, making them potential orthogonal reagents for sandwich immunoassays. These findings serve as a starting point for the development of SARS-CoV-2 diagnostics or conjugates for virus-directed delivery of therapeutics.

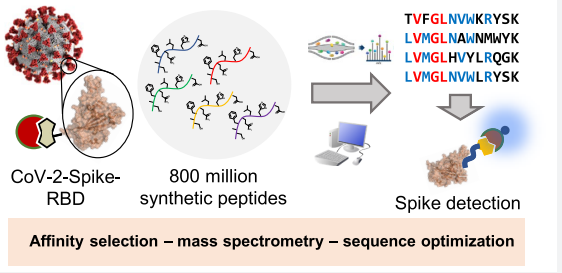

INTRODUCTION

Since the end of 2019, the severe acute respiratory syndrome coronavirus 2 (SARS-CoV-2) has caused the global coronavirus disease 2019 (COVID-19) pandemic. With 30 million cases and over 950 000 deaths (by August 2020), SARS-CoV-2 has spread further than SARS-CoV-1 or middle east respiratory syndrome (MERS-CoV).[1,2] There is a need for diagnostic testing of SARS-CoV-2 to improve containment.[3,4] Currently, the reverse-transcriptase polymerase chain reaction (RT-PCR) method is the gold standard of SARS-CoV-2 detection.[5,6] Serologic detection of patient-derived antibodies can be used to track SARS-CoV-2 progression and immunity but has limited early detection ability.[6−8] Direct detection of SARS-CoV-2 has been proposed in scalable, rapidly deployed formats but often suffers from low sensitivity that limits effectivity in general population testing.[9,10] Thus, the discovery of additional reagents to enable early and rapid SARS-CoV-2 detection and/or neutralization is critical.

Recognition of viral surface proteins by high-affinity reagents represents a promising strategy for virus detection or neutralization. Coronaviruses display multiple copies of spike protein on their surface.[11,12] SARS-CoV-2 (as well as SARS-CoV-1) binds with high affinity to human angiotensin converting enzyme 2 (ACE2) receptors as a primary mechanism for initiating cell invasion.[13,14] Several proteins that target the SARS-CoV-2 spike have been described. Soluble human and modified ACE2 show a high affinity to the SARS-CoV-2 spike protein receptor binding domain (RBD) and neutralizing activity in live virus infection models.[15,16] Computational design led to the discovery of high-affinity miniprotein binders for RBD.[17] Also, numerous neutralizing antibodies and nanobodies binding to the SARS-CoV-2-spike-RBD have been described.[18,19]

Peptide sequences with high affinity and selectivity for the SARS-CoV-2 spike protein and its RBD could be advanced for the development of new diagnostic or therapeutic modalities. Peptides have been previously investigated as potential SARS-CoV-2 antiviral agents. For example, α-helical peptides binding to the S2 unit of the coronavirus spike protein have been described as potent fusion inhibitors.[20] Computational and experimental studies supported targeting the spike RBD with linear peptides derived from the ACE2 N-terminus.[21,22] Investigations in our laboratory, however, indicated that peptides up to 23 residues in length derived from the ACE2 N-terminus do not associate with high affinity to SARS-CoV-2-spike-RBD expressed and isolated from human cells.[23] With straightforward handling, preparation, and late-stage modification,[24−26] peptides are attractive potential candidates for point-of-care diagnostics.

Received: September 28, 2020
Published: December 18, 2020

https://dx.doi.org/10.1021/acscentsci.0c01309
ACS Cent. Sci. 2021, 7, 156−163

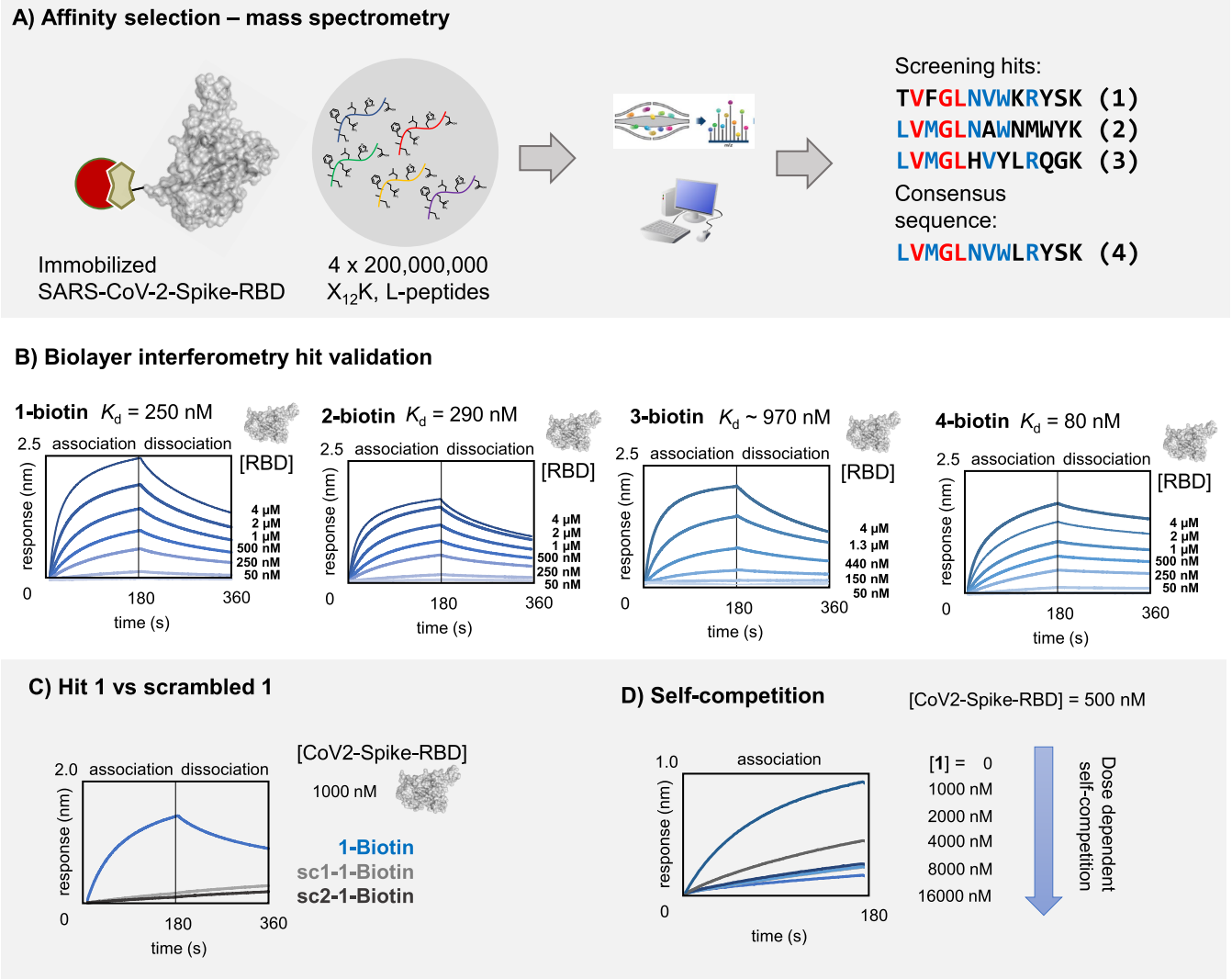

Figure 1. SARS-CoV-2-spike-RBD binding peptides with nanomolar affinity were identified by affinity selection–mass spectrometry. (A) Schematic representation of the AS–MS workflow and enriched sequences. In brief, biotinylated SARS-CoV-2-spike-RBD was immobilized on magnetic streptavidin beads and then incubated with peptide libraries. Unbound members were removed by washing. Peptides bound to SARS-CoV-2-spike-RBD were eluted and analyzed by nanoLC–MS/MS. (B) BLI curves for association/dissociation of peptides **1**–**4** to SARS-CoV-2-spike-RBD (in kinetic buffer: 1× PBS, pH = 7.2, 0.1% bovine serum albumin, 0.02% Tween-20). While peptide **4** had higher affinity, peptide **1**, compared to **2** and **4**, had the best solubility and was used for all further investigations. Peptides **2** and **4** precipitated from solution within hours at concentrations greater than 10 μM. Kinetic binding results are reported in Table S1. (C) BLI curves for **1** (blue line) and scrambled analogues of **1** (light and dark gray lines, respectively; sc1, GSVKRWLTYVKNFK; and sc2, RFYVTKGWSNKVLK). (D) Self-competition analysis (BLI association) of **1** to SARS-CoV-2-spike-RBD: peptide **1-biotin** immobilized on BLI tips was dipped into solutions containing SARS-CoV-2-spike-RBD and **1** ([RBD] = 500 nM; [**1**] = 0–16 μM). Increasing the concentration of **1** in solution causes less free RBD available in solution (due to RBD-**1** complex formation) and results in a concentration-dependent decrease in BLI response.

Here, we report the discovery of synthetic peptides (13 residues) with nanomolar affinity for the SARS-CoV-2-spike-RBD. We leveraged a combinatorial affinity selection–mass spectrometry (AS–MS) platform[27] for the rapid identification of sequences with high affinity and selectivity toward RBD over human proteins. After chemical synthesis of the identified peptides, validation of their binding activity was observed using biolayer interferometry (BLI) and a magnetic bead pull-down assay. In an enzyme-linked immunosorbent assay (ELISA), these peptides detected RBD after addition to a complex biological matrix.

RESULTS AND DISCUSSION

Peptides with a shared sequence motif were identified by affinity selection–mass spectrometry (AS–MS). SARS-CoV-2-spike-RBD was biotinylated and immobilized on streptavidin-coated magnetic beads. Following an AS–MS protocol recently established by our group,[27,28] we screened four ~200 million member peptide libraries against the immobilized spike RBD (the peptide libraries were synthesized and characterized as previously described[27]). The peptide library design was $X_{12}K$, where X = any canonical amino acid except Ile and Cys. In parallel, with the same library, we performed an enrichment with the anti-hemagglutinin monoclonal antibody 12ca5 to identify nonspecific binders, which would appear in both selections. Unbound peptides were removed by three

https://dx.doi.org/10.1021/acscentsci.0c01309
ACS Cent. Sci. 2021, 7, 156–163

washes with 1× PBS; potential binders were eluted with the denaturant guanidinium hydrochloride and analyzed by nano-liquid-chromatography−tandem mass spectrometry (nanoLC−MS/MS). The resultant MS spectra were visualized with the sequencing software PEAKS 8.5 and further refined with a Python script that nominated variants matching the library design.[29]

From the ∼800 million screened peptides, three peptide sequences were identified (**1**−**3**, Figure 1a). An extracted ion chromatogram was generated for the target mass of each peptide, revealing that each was selectively enriched against the SARS-CoV-2-spike-RBD and not the 12ca5 off-target control (Figures S2−S4). The three identified peptides shared a common motif at the N-terminus: *V*GL (red letters in Figure 1A). For the additional six positions, we observed enrichment for specific residues as indicated by blue letters (Figure 1A). Based on the similarity of the three sequences, the residues with the highest positional frequencies were combined resulting in the consensus sequence (**4**, Figure 1a).

The identified peptide sequences bound SARS-CoV-2-spike-RBD with nanomolar affinity. To validate the identified sequences, we synthesized biotinylated peptides **1**−**4**. The compounds were immobilized on streptavidin-coated biolayer interferometry (BLI) tips and used to measure association and dissociation of SARS-CoV-2-spike-RBD at different concentrations. Peptides **1**−**3** bound the SARS-CoV-2-spike-RBD with apparent dissociation constants, K_d, of 250, 290, and 970 nM, respectively (Figure 1B). The consensus peptide **4** bound the SARS-CoV-2-spike-RBD with K_d = 80 nM, a ∼3-fold improvement over the originally identified hit peptide **1** (Figure 1B). To determine whether the binding is sequence-specific, two scrambled variants of peptide **1** (sc1 and sc2) were prepared and tested by BLI, and no association was observed in either case (Figure 1C). We also tested the association of peptide **1** to 12ca5 and observed minimal association especially when compared directly to a known positive control 12ca5 binder (Figure S5). While peptide **4** had the highest affinity to SARS-CoV-2-spike-RBD, peptide **1** was the most soluble and was used for all further investigations.

Peptide **1** associates to a specific site on the SARS-CoV-2-spike-RBD as determined by a self-competition binding assay. We immobilized peptide **1-biotin** on BLI tips and dipped them into solutions containing SARS-CoV-2-spike-RBD and peptide **1** ([RBD] = 500 nM; [**1**] = 0−16 μM). With an increasing concentration of peptide **1** in solution, we observed a concentration-dependent decrease in binding. With less free RBD available in solution, less RBD associates to the BLI tip coated in peptide **1** (Figure 1C).

Peptide **1** does not interfere with ACE2 binding to the RBD. For this experiment, we immobilized ACE2 on BLI tips and dipped them into solutions of SARS-CoV-2-spike-RBD and peptide **1** ([RBD] = 100 nM; [**1**] = 0−62 μM, Figure S6). We did not observe a decrease in binding response. This can be explained by the fact that peptide **1** does not have sufficient affinity to block binding of RBD to ACE2 or that peptide **1** might bind to a site on the RBD separate from ACE2. In the latter case, ACE2 and peptide **1-biotin** might form an orthogonal ligand pair useful for spike-RBD sandwich immunoassays.

Alanine scanning mutagenesis of sequence **1** was used to determine the importance of the common motif (*V*GL) and other residues in binding to RBD (Figure 2). Mutations V2A and G4A decreased binding to SARS-CoV-2-spike-RBD,

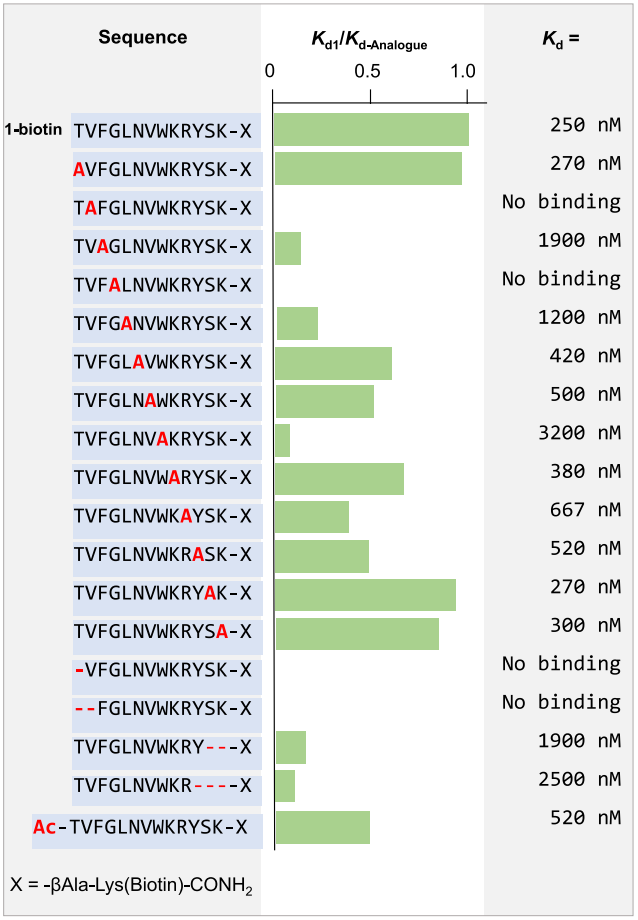

Figure 2. Alanine scanning and sequence truncations of **1** reveal binding hotspots. Binding to SARS-CoV-2-spike-RBD of alanine mutants and truncated peptides was measured by BLI as detailed in Figure 1. Ratios between binding of original sequence **1** and each mutant, respectively, are shown as green bars. Individual steady state K_d values are shown in the right column. Kinetic binding results are reported in Table S1.

confirming their contributions to the motif identified (Figure 2). Mutations of hydrophobic residues reduced the peptide binding affinity. Specifically, the mutants F3A, L5A, and W8A decreased the binding by 5- to 13-fold. Position 3 in the other identified peptides contained a methionine suggesting that a hydrophobic residue is important at this site. Similarly, position 8 needs to be either tryptophan or tyrosine, indicating that an aromatic group is important.

To assess the importance of sequence length, we synthesized N-terminal and C-terminal truncations of peptide **1**. A one residue truncation from the N-terminus abolished binding, confirming the frame dependency of the binding motif. N-terminal acetylation reduced the binding affinity to K_d = 520 nM, indicating that the N-terminal amino group is important. Truncations from the C-terminus decreased binding ∼10-fold.

Peptide **1** binds to the spike proteins of SARS-CoV-1 and MERS-CoV coronaviruses. Patient-derived antibodies often bind SARS-CoV-1 and SARS-CoV-2 selectively, with less binding activity against MERS-CoV.[30] However, the spike protein shares some degree of sequence and structural similarity among several species of the β-coronavirus family.[31] We tested the binding of peptide **1** to the RBDs of SARS-CoV-1 and MERS-CoV and observed a K_d of 600 and 120 nM,

https://dx.doi.org/10.1021/acscentsci.0c01309
ACS Cent. Sci. 2021, 7, 156−163

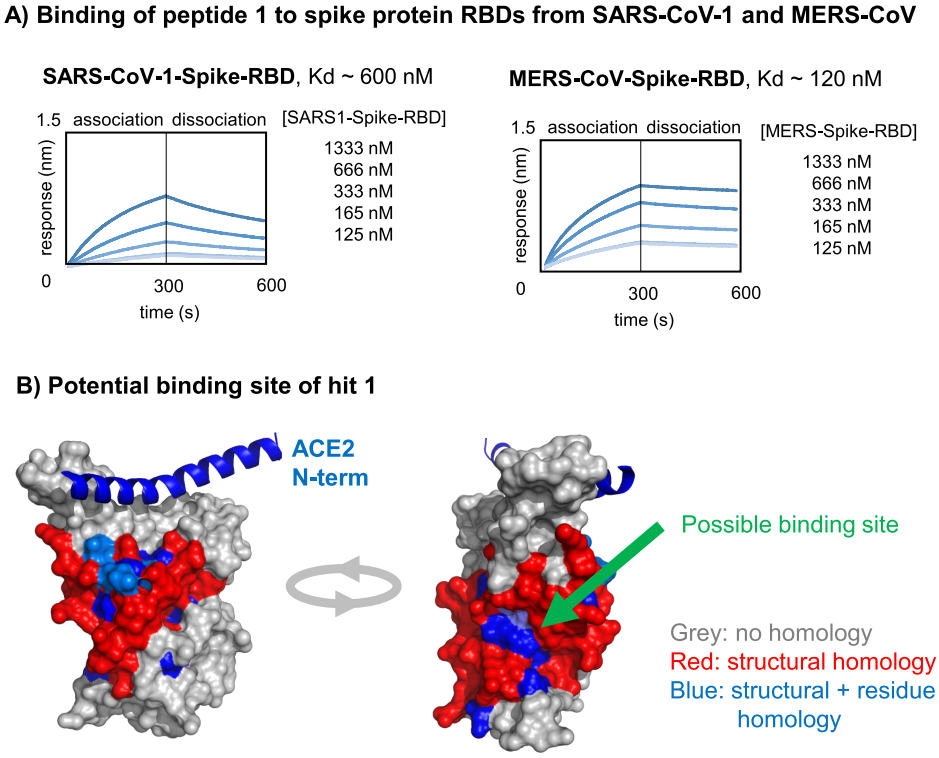

Figure 3. Peptide **1** binds to SARS-CoV-1-spike-RBD and MERS-CoV-spike-RBD. (A) The binding of peptide **1-biotin** to SARS-CoV-1-spike-RBD and MERS-CoV-spike-RBD was determined by BLI. (B) A structural overlay of SARS-CoV-2-spike-RBD and MERS-CoV-spike-RBD was performed with the software PyMol (using PDB structures 6vw1 and 6c6z). Regions with the homology of the secondary structure between the two proteins are colored in red. The homologous regions were manually analyzed to identify positions with identical residues in both proteins: blue. Since peptide **1-biotin** binds to both with comparable affinity, the binding site could potentially be in a region with high homology.

respectively (Figure 3A). The K_d values are the same order of magnitude as the binding of peptide **1** to SARS-CoV-2-spike-RBD.

We also investigated the binding of peptide **1** to the spike protein of HKU1, which is an endemic human coronavirus.[30,32] Since the receptor-binding domain of this protein was not commercially available, we compared the binding of peptide **1** to the HKU1 spike S1 protein subunit and to the SARS-CoV-2 spike S1 protein subunit (both expressed in mammalian cells). The binding of peptide **1** to SARS-CoV-2-S1 demonstrated a K_d of 40 nM but showed considerably weaker association to the HKU1-S1 protein (Figure S7). The stronger binding affinity of peptide **1** to SARS-CoV-2-S1 (40 nM) compared to SARS-CoV-2-spike-RBD (250 nM) could arise from reduced conformational freedom of the RBD as a part of the S1 spike protein compared to the RBD alone. Alternatively, the difference could be explained by potential variability in quality of recombinant expression of the different commercial proteins. In addition, we confirmed binding of peptide **1-biotin** to the SARS-CoV-2-spike trimer (Figure S7). The association intensity (comparable to the one determined using ACE2-biotin) shows that peptide **1-biotin** can bind also the full length SARS-CoV-2-spike trimer.

Significant binding was observed with MERS-CoV and peptide **1**, suggesting that a similar binding site might be recognized. We were intrigued by the retained binding affinity of peptide **1** to MERS-CoV as SARS-CoV-1, SARS-CoV-2, and MERS-CoV RBDs have a high level of structural homology. On a residue level, however, only SARS-CoV-1 and SARS-CoV-2 share a high level of sequence homology (~74%) while MERS-CoV and SARS-CoV-2-spike-RBDs share only ~24%. Analyzing the overlay of these proteins via PyMOL, we found only two patches with residue homology large enough to associate with a peptide binder (colored in blue in Figure 3B, sequence alignment in Figure S12). One of these patches is located in proximity to the ACE2 binding site and the other on the opposite side of the RBD. Since no perturbation of the ACE2 binding to RBD was observed in the presence of peptide **1**, the patch on the opposite side of the RBD is suggested as a possible binding site for peptide **1**.

SARS-CoV-2-spike-RBD can be selectively enriched from human serum proteins using immobilized peptide **1**. To investigate the binding specificity of **1** to RBD in a biological matrix, we added SARS-CoV-2-spike-RBD to human serum (10% in 1× PBS) and incubated with magnetic beads displaying peptide **1-biotin** (Figure 4A). We removed the supernatant, washed the beads, and treated with urea to elute bound proteins. We analyzed the urea fraction by SDS-PAGE and observed selective enrichment of SARS-CoV-2-spike-RBD; no other proteins were detected (Figure 4B). The selective binding of peptide **1** to SARS-CoV-2-spike-RBD and isolation from complex biological media point toward potential diagnostic applications or the use of this peptide as a delivery agent for antiviral payloads.

Nanomolar to picomolar concentrations of RBD in a biological matrix were detected by peptide **1-biotin** in an enzyme-linked immunosorbent assay (ELISA) format. We performed an ELISA by immobilizing different concentrations of RBD (100 nM to 100 fM) mixed with fetal bovine serum (FBS) onto the ELISA plate. We then added peptide **1-biotin**

https://dx.doi.org/10.1021/acscentsci.0c01309
ACS Cent. Sci. 2021, 7, 156−163

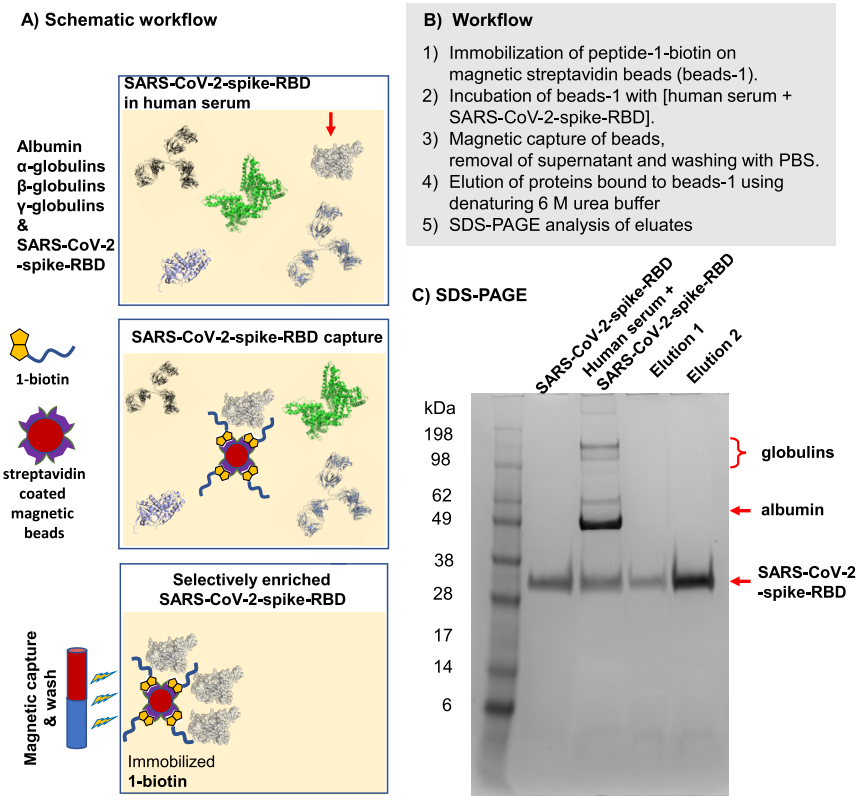

Figure 4. SARS-CoV-2-spike-RBD can be selectively enriched from human serum proteins. (A) Schematic representation of the pull-down of SARS-CoV-2-spike-RBD from human serum. (B) Workflow: spike RBD was added to human serum (RBD: 0.27 mg/mL, 10% human serum, 1× PBS), and the mix was incubated with magnetic beads (MyOne Dynabeads) displaying peptide **1-biotin** (1 h, 4 °C). The supernatant (containing nonbinding proteins) was removed, and the beads were washed with 1× PBS (3 × 1 mL). Bound proteins were eluted with 6 M urea (elution 1:50 μL, 30 s; elution 2:50 μL, 120 s) and analyzed by SDS PAGE (C). The gel shows (from left to right) (1) molecular weight ladder; (2) purified SARS-CoV-2-spike-RBD (1 μg); (3) human serum mixed with SARS-CoV-2-spike-RBD; (4) elution 1 (30 μL of elution sample 1); and (5) elution 2 (30 μL of elution sample 2). The analysis was performed using BoltTM 4−12% Bis-Tris Plus gels (10-wells), 165 V for 36 min, utilizing prestained Invitrogen SeeBlueTM Plus2 molecular weight standard with BoltTM LDS sample buffer (4×).

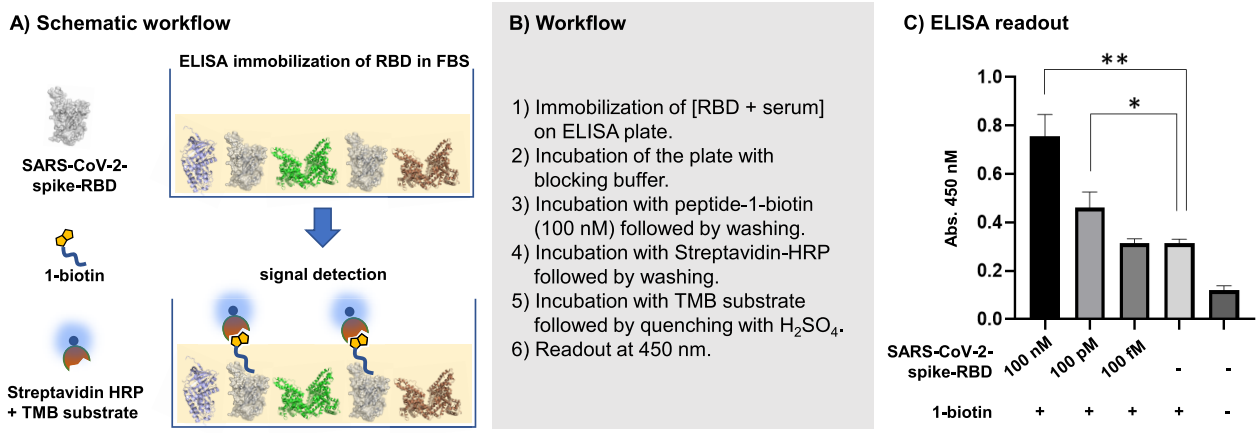

Figure 5. Picomolar SARS-CoV-2-spike-RBD quantities were detected by ELISA. (A) Schematic representation of the ELISA assay. (B) Workflow: Serial dilutions (100 nM to 100 fM) of RBD mixed with fetal bovine serum (FBS) were immobilized on an ELISA plate. The plate was incubated with peptide **1-biotin**, followed by streptavidin-HRP and TMB substrate. (C) ELISA absorbance readout at 450 nM as a function of RBD concentrations. Measurements were performed in technical triplicates (n = 3), and statistical significance was calculated with the unpaired t test. RBD 100 nM vs no RBD, p = 0.0012 (**); RBD 100 pM vs no RBD, p = 0.018 (*).

(100 nM) to each well and subsequently streptavidin-HRP (horseradish peroxidase) and tetramethylbenzidine (TMB) substrate (Figure 5A). We detected SARS-CoV-2-spike-RBD at 100 nM and 100 pM concentrations with a signal significantly stronger than the background (Figure 5B and Figure S10). Initial experiments with SARS-CoV-2-spike-RBD dissolved in human serum also resulted in a dose response detection with a significant signal at a nanomolar RBD concentration (Figure S11). The background signal caused by the peptide in absence of RBD on the plate could be caused by

https://dx.doi.org/10.1021/acscentsci.0c01309
ACS Cent. Sci. 2021, 7, 156−163

nonspecific binding of peptide **1-biotin** to components of the biological matrix. For a potential use as a diagnostic tool, further refinement of the detection conditions will be necessary. We tested the stability of peptide **1-biotin** in human serum and found minimal degradation in conditions comparable to the ELISA (Figure S13).

Safety Statement. No unexpected or unusually high safety hazards were encountered.

CONCLUDING REMARKS

Taken together, we have shown the use of an affinity selection−mass spectrometry platform[27] for the rapid discovery of peptides binding to the SARS-CoV-2-spike-RBD. From 800 million synthetic peptides screened, we identified three motif-bearing sequences that have nanomolar affinity. These peptides bind SARS-CoV-2-spike-RBD with selectivity over multiple human serum proteins and could detect it at nanomolar to picomolar concentrations in an ELISA format. Cross-binding of peptide **1** to the MERS-CoV coronavirus spike protein indicated a possible binding site distal from the binding site for the human ACE2 receptor.

The peptides reported here are potential starting points for the development of affinity-based diagnostic tools.[33−35] High-affinity reagents without direct competition activity for native receptors could be used for virus-directed delivery of antiviral payloads, or for the development of proteasome or lysosome targeting chimeras (PROTACs[36,37] and LYTACs[38]). Adapting peptide **1** to a chemiluminescence enzyme immunoassay or a similar assay could improve its sensitivity for detection of SARS-CoV-2.[8,39] Because of its selectivity in biological media, peptide **1** could be utilized for the direct detection of SARS-CoV-2 in bodily fluids. Improved diagnostics are a topic of intense COVID-19 research as they may provide rapid, reliable, and early detection.[40] While direct detection suffers from low sensitivity,[10,41] the rapid identification of SARS-CoV-2 is critical for patient contact tracing, identifying hosts, and epidemiologic studies.[2−4] The peptides discovered by our platform may provide a useful SARS-CoV-2 detection modality to help achieve these goals.

ASSOCIATED CONTENT

Supporting Information

The Supporting Information is available free of charge at https://pubs.acs.org/doi/10.1021/acscentsci.0c01309.

Synthesis and experimental procedures as well as characterization of all compounds and libraries (PDF)

AUTHOR INFORMATION

Corresponding Author

Bradley L. Pentelute − *Department of Chemistry, The Koch Institute for Integrative Cancer Research, and Center for Environmental Health Sciences, Massachusetts Institute of Technology, Cambridge, Massachusetts 02139, United States; Broad Institute of MIT and Harvard, Cambridge, Massachusetts 02142, United States;* orcid.org/0000-0002-7242-801X; Email: blp@mit.edu

Authors

Sebastian Pomplun − *Department of Chemistry, Massachusetts Institute of Technology, Cambridge, Massachusetts 02139, United States*

Muhammad Jbara − *Department of Chemistry, Massachusetts Institute of Technology, Cambridge, Massachusetts 02139, United States;* orcid.org/0000-0002-4206-5908

Anthony J. Quartararo − *Department of Chemistry, Massachusetts Institute of Technology, Cambridge, Massachusetts 02139, United States*

Genwei Zhang − *Department of Chemistry, Massachusetts Institute of Technology, Cambridge, Massachusetts 02139, United States*

Joseph S. Brown − *Department of Chemistry, Massachusetts Institute of Technology, Cambridge, Massachusetts 02139, United States;* orcid.org/0000-0002-8145-800X

Yen-Chun Lee − *Department of Chemistry, Massachusetts Institute of Technology, Cambridge, Massachusetts 02139, United States*

Xiyun Ye − *Department of Chemistry, Massachusetts Institute of Technology, Cambridge, Massachusetts 02139, United States*

Stephanie Hanna − *Department of Chemistry, Massachusetts Institute of Technology, Cambridge, Massachusetts 02139, United States*

Complete contact information is available at: https://pubs.acs.org/10.1021/acscentsci.0c01309

Notes

The authors declare the following competing financial interest(s): B.L.P. is a cofounder of Amide Technologies and Resolute Bio. Both companies focus on the development of protein and peptide therapeutics.

ACKNOWLEDGMENTS

This research was supported by a COVID-19 Fast Grant award sponsored by Emergent Ventures at the Mercatus Center, George Mason University, and by a Bristol-Myers Squibb Unrestricted Grant in Synthetic Organic Chemistry awarded to B.L.P. S.P. thanks the Deutsche Forschungsgemeinschaft for a postdoctoral fellowship (DFG, PO 2413/1-1). Y.-C.L. is supported by the Deutsche Forschungsgemeinschaft (DFG, LE 4224/1-1). M.J. gratefully acknowledges postdoctoral fellowship support from the Rothschild Foundation, the Fulbright Program, and the Israel Council for Higher Education (VATAT). We thank the Biophysical Instrumentation Facility at MIT for providing access to the Octet Red96 Bio-Layer Interferometry System (NIH S10OD016326). We gratefully acknowledge Andrei Loas for helping with the preparation of the manuscript and organizational support during the project. We gratefully acknowledge the Center for Disease Control for the public domain image of the SARS-CoV-2 particle, used in our TOC graphic.

ABBREVIATIONS

ELISA, enzyme-linked immunosorbent assay; SARS-CoV, severe acute respiratory syndrome coronavirus; Covid-19, coronavirus disease 19; RT-PCR, reverse transcriptase polymerase chain reaction; MERS-CoV, middle east respiratory syndrome; ACE2, angiotensin converting enzyme 2; RBD, receptor binding domain; SDS-PAGE, sodium dodecyl sulfate−polyacrylamide gel electrophoresis

REFERENCES

(1) World Health Organization. *Coronavirus Disease (COVID-19) Weekly Epidemiological Update for August 31st 2020*; WHO, 2020.

(2) Webb Hooper, M.; Nápoles, A. M.; Pérez-Stable, E. J. COVID-19 and Racial/Ethnic Disparities. *JAMA* **2020**, *323* (24), 2466.
(3) Tromberg, B. J.; Schwetz, T. A.; Pérez-Stable, E. J.; Hodes, R. J.; Woychik, R. P.; Bright, R. A.; Fleurence, R. L.; Collins, F. S. Rapid Scaling Up of Covid-19 Diagnostic Testing in the United States — The NIH RADx Initiative. *N. Engl. J. Med.* **2020**, *383* (11), 1071−1077.
(4) Carter, L. J.; Garner, L. V.; Smoot, J. W.; Li, Y.; Zhou, Q.; Saveson, C. J.; Sasso, J. M.; Gregg, A. C.; Soares, D. J.; Beskid, T. R.; Jervey, S. R.; Liu, C. Assay Techniques and Test Development for COVID-19 Diagnosis. *ACS Cent. Sci.* **2020**, *6* (5), 591−605.
(5) Zou, L.; Ruan, F.; Huang, M.; Liang, L.; Huang, H.; Hong, Z.; Yu, J.; Kang, M.; Song, Y.; Xia, J.; Guo, Q.; Song, T.; He, J.; Yen, H.-L.; Peiris, M.; Wu, J. SARS-CoV-2 Viral Load in Upper Respiratory Specimens of Infected Patients. *N. Engl. J. Med.* **2020**, *382* (12), 1177−1179.
(6) Sethuraman, N.; Jeremiah, S. S.; Ryo, A. Interpreting Diagnostic Tests for SARS-CoV-2. *JAMA - J. Am. Med. Assoc.* **2020**, *323* (22), 2249−2251.
(7) GeurtsvanKessel, C. H.; Okba, N. M. A.; Igloi, Z.; Bogers, S.; Embregts, C. W. E.; Laksono, B. M.; Leijten, L.; Rokx, C.; Rijnders, B.; Rahamat-Langendoen, J.; van den Akker, J. P. C.; van Kampen, J. J. A.; van der Eijk, A. A.; van Binnendijk, R. S.; Haagmans, B.; Koopmans, M. An Evaluation of COVID-19 Serological Assays Informs Future Diagnostics and Exposure Assessment. *Nat. Commun.* **2020**, *11* (1), 1−5.
(8) Long, Q. X.; Liu, B. Z.; Deng, H. J.; Wu, G. C.; Deng, K.; Chen, Y. K.; Liao, P.; Qiu, J. F.; Lin, Y.; Cai, X. F.; Wang, D. Q.; Hu, Y.; Ren, J. H.; Tang, N.; Xu, Y. Y.; Yu, L. H.; Mo, Z.; Gong, F.; Zhang, X. L.; Tian, W. G.; Hu, L.; Zhang, X. X.; Xiang, J. L.; Du, H. X.; Liu, H. W.; Lang, C. H.; Luo, X. H.; Wu, S. B.; Cui, X. P.; Zhou, Z.; Zhu, M. M.; Wang, J.; Xue, C. J.; Li, X. F.; Wang, L.; Li, Z. J.; Wang, K.; Niu, C. C.; Yang, Q. J.; Tang, X. J.; Zhang, Y.; Liu, X. M.; Li, J. J.; Zhang, D. C.; Zhang, F.; Liu, P.; Yuan, J.; Li, Q.; Hu, J. L.; Chen, J.; Huang, A. L. Antibody Responses to SARS-CoV-2 in Patients with COVID-19. *Nat. Med.* **2020**, *26* (6), 845−848.
(9) Nagura-Ikeda, M.; Imai, K.; Tabata, S.; Miyoshi, K.; Murahara, N.; Mizuno, T.; Horiuchi, M.; Kato, K.; Imoto, Y.; Iwata, M.; Mimura, S.; Ito, T.; Tamura, K.; Kato, Y. Clinical Evaluation of Self-Collected Saliva by Quantitative Reverse Transcription-PCR (RT-QPCR), Direct RT-QPCR, Reverse Transcription-Loop-Mediated Isothermal Amplification, and a Rapid Antigen Test To Diagnose COVID-19. *J. Clin. Microbiol.* **2020**, *58* (9), 1−9.
(10) Scohy, A.; Anantharajah, A.; Bodéus, M.; Kabamba-Mukadi, B.; Verroken, A.; Rodriguez-Villalobos, H. Low Performance of Rapid Antigen Detection Test as Frontline Testing for COVID-19 Diagnosis. *J. Clin. Virol.* **2020**, *129* (May), 104455.
(11) Yuan, M.; Wu, N. C.; Zhu, X.; Lee, C. C. D.; So, R. T. Y.; Lv, H.; Mok, C. K. P.; Wilson, I. A. A Highly Conserved Cryptic Epitope in the Receptor Binding Domains of SARS-CoV-2 and SARS-CoV. *Science (Washington, DC, U. S.)* **2020**, *368* (6491), 630−633.
(12) Wrapp, D.; Wang, N.; Corbett, K. S.; Goldsmith, J. A.; Hsieh, C. L.; Abiona, O.; Graham, B. S.; McLellan, J. S. Cryo-EM Structure of the 2019-NCoV Spike in the Prefusion Conformation. *Science (Washington, DC, U. S.)* **2020**, *367* (6483), 1260−1263.
(13) Wang, Q.; Zhang, Y.; Wu, L.; Niu, S.; Song, C.; Zhang, Z.; Lu, G.; Qiao, C.; Hu, Y.; Yuen, K. Y.; Wang, Q.; Zhou, H.; Yan, J.; Qi, J. Structural and Functional Basis of SARS-CoV-2 Entry by Using Human ACE2. *Cell* **2020**, *181* (4), 894−904.
(14) Lan, J.; Ge, J.; Yu, J.; Shan, S.; Zhou, H.; Fan, S.; Zhang, Q.; Shi, X.; Wang, Q.; Zhang, L.; Wang, X. Structure of the SARS-CoV-2 Spike Receptor-Binding Domain Bound to the ACE2 Receptor. *Nature* **2020**, *581* (7807), 215−220.
(15) Monteil, V.; Kwon, H.; Prado, P.; Hagelkrüys, A.; Wimmer, R. A.; Stahl, M.; Leopoldi, A.; Garreta, E.; Hurtado del Pozo, C.; Prosper, F.; Romero, J. P.; Wirnsberger, G.; Zhang, H.; Slutsky, A. S.; Conder, R.; Montserrat, N.; Mirazimi, A.; Penninger, J. M. Inhibition of SARS-CoV-2 Infections in Engineered Human Tissues Using Clinical-Grade Soluble Human ACE2. *Cell* **2020**, *181* (4), 905−913.
(16) Chan, K. K.; Dorosky, D.; Sharma, P.; Abbasi, S. A.; Dye, J. M.; Kranz, D. M.; Herbert, A. S.; Procko, E. Engineering Human ACE2 to Optimize Binding to the Spike Protein of SARS Coronavirus 2. *Science* **2020**, *369* (6508), 1261−1265.
(17) Cao, L.; Goreshnik, I.; Coventry, B.; Case, J. B.; Miller, L.; Kozodoy, L.; Chen, R. E.; Carter, L.; Walls, A. C.; Park, Y.; Strauch, E.; Stewart, L.; Diamond, M. S.; Veesler, D.; Baker, D. De Novo Design of Picomolar SARS-CoV-2 miniprotein Inhibitors. *Science* **2020**, *370* (6515), 426−431.
(18) Wu, Y.; Li, C.; Xia, S.; Tian, X.; Kong, Y.; Wang, Z.; Gu, C.; Zhang, R.; Tu, C.; Xie, Y.; Yang, Z.; Lu, L.; Jiang, S.; Ying, T. Identification of Human Single-Domain Antibodies against SARS-CoV-2. *Cell Host Microbe* **2020**, *27*, 891−898.
(19) Wrapp, D.; Vlieger De, D.; Corbett, K. S.; Torres, G. M.; Breedam van, W.; Roose, K.; Schie van, L.; Team, V.-C. C. R.; Hoffmann, M.; Pöhlmann, S.; Graham, B. S.; Callewaert, N.; Schepens, B.; Saelens, X.; McLellan, J. S. Structural Basis for Potent Neutralization of Betacoronaviruses by Single-Domain Camelid Antibodies. *Cell* **2020**, *181*, 1004.
(20) Xia, S.; Liu, M.; Wang, C.; Xu, W.; Lan, Q.; Feng, S.; Qi, F.; Bao, L.; Du, L.; Liu, S.; Qin, C.; Sun, F.; Shi, Z.; Zhu, Y.; Jiang, S.; Lu, L. Inhibition of SARS-CoV-2 (Previously 2019-NCoV) Infection by a Highly Potent Pan-Coronavirus Fusion Inhibitor Targeting Its Spike Protein That Harbors a High Capacity to Mediate Membrane Fusion. *Cell Res.* **2020**, *30* (4), 343−355.
(21) Han, Y.; Král, P. Computational Design of ACE2-Based Peptide Inhibitors of SARS-CoV-2. *ACS Nano* **2020**, *14* (4), 5143−5147.
(22) Han, D. P.; Penn-Nicholson, A.; Cho, M. W. Identification of Critical Determinants on ACE2 for SARS-CoV Entry and Development of a Potent Entry Inhibitor. *Virology* **2006**, *350* (1), 15−25.
(23) Zhang, G.; Pomplun, S.; Loftis, A. R.; Tan, X.; Loas, A.; Pentelute, B. L. Investigation of ACE2 N-Terminal Fragments Binding to SARS-CoV-2 Spike RBD. *BioRXiv*, 2020.03.19.999318v2, 2020. DOI: 10.1101/2020.03.19.999318v2.
(24) Touti, F.; Gates, Z. P.; Bandyopdhyay, A.; Lautrette, G. In-Solution Enrichment Identifies Peptide Inhibitors of Protein - Protein Interactions Protein-Protein Interactions. *Nat. Chem. Biol.* **2019**, *15*, 410−418.
(25) Nevola, L.; Giralt, E. Modulating Protein-Protein Interactions: The Potential of Peptides. *Chem. Commun.* **2015**, *51* (16), 3302−3315.
(26) London, N.; Movshovitz-Attias, D.; Schueler-Furman, O. The Structural Basis of Peptide-Protein Binding Strategies. *Structure* **2010**, *18* (2), 188−199.
(27) Quartararo, A. J.; Gates, Z. P.; Somsen, B. A.; Hartrampf, N.; Ye, X.; Shimada, A.; Kajihara, Y.; Ottman, C.; Pentelute, B. L. Ultra-Large Chemical Libraries for the Discovery of High-Affinity Peptide Binders. *Nat. Commun.* **2020**, *11* (1), 3183.
(28) Pomplun, S.; Gates, Z. P.; Zhang, G.; Quartararo, A. J.; Pentelute, B. L. Discovery of Nucleic Acid Binding Molecules from Combinatorial Biohybrid Nucleobase Peptide Libraries. *J. Am. Chem. Soc.* **2020**, *142* (46), 19642.
(29) Vinogradov, A.; Gates, Z. P.; Zhang, C.; Quartararo, A. J.; Halloran, K. H.; Pentelute, B. L. Library Design-Facilitated High-Throughput Sequencing of Synthetic Peptide Libraries. *ACS Comb. Sci.* **2017**, *19* (11), 694−701.
(30) Okba, N. M. A.; Müller, M. A.; Li, W.; Wang, C.; Geurtsvankessel, C. H.; Corman, V. M.; Lamers, M. M.; Sikkema, R. S.; Bruin De, E.; Chandler, F. D.; Yazdanpanah, Y.; Hingrat, Q. Le; Descamps, D.; Houhou-Fidouh, N.; Reusken, C. B. E. M.; Bosch, B. J.; Drosten, C.; Koopmans, M. P. G.; Haagmans, B. L. Severe Acute Respiratory Syndrome Coronavirus 2-Specific Antibody Responses in Coronavirus Disease Patients. *Emerging Infect. Dis.* **2020**, *26* (7), 1478−1488.
(31) Li, F. Structure, Function, and Evolution of Coronavirus Spike Proteins. *Annu. Rev. Virol.* **2016**, *3*, 237−261.
(32) Pyrc, K.; Berkhout, B.; van der Hoek, L. The Novel Human Coronaviruses NL63 and HKU1. *J. Virol.* **2007**, *81* (7), 3051−3057.

(33) Hurwitz, A. M.; Huang, W.; Estes, M. K.; Atmar, R. L.; Palzkill, T. Deep Sequencing of Phage-Displayed Peptide Libraries Reveals Sequence Motif That Detects Norovirus. *Protein Eng., Des. Sel.* **2017**, *30* (2), 129−139.
(34) Cretich, M.; Gori, A.; D'Annessa, I.; Chiari, M.; Colombo, G. Peptides for Infectious Diseases: From Probe Design to Diagnostic Microarrays. *Antibodies* **2019**, *8* (1), 23.
(35) Edward Williams, M.; Tincho, M. Molecular Validation of Putative Antimicrobial Peptides for Improved Human Immunodeficiency Virus Diagnostics via HIV Protein P24. *J. AIDS Clin. Res.* **2016**, *07* (05), 1000571.
(36) Paiva, S. L.; Crews, C. M. Targeted Protein Degradation: Elements of PROTAC Design. *Curr. Opin. Chem. Biol.* **2019**, *50*, 111−119.
(37) Chatterjee, P.; Ponnapati, M.; Jacobson, J. M. Targeted Intracellular Degradation of SARS-CoV-2 RBD via Computationally-Optimized Peptide Fusions. *Science* **2020**, *3* (1), 715.
(38) Banik, S. M.; Pedram, K.; Wisnovsky, S.; Riley, N. M.; Bertozzi, C. R. Lysosome Targeting Chimeras for the Degradation of Secreted and Membrane Proteins. *ChemRxiv*, 7927061.v2, 2019. https://doi.org/10.26434/chemrxiv.7927061.v2.
(39) Kyosei, Y.; Namba, M.; Yamura, S.; Takeuchi, R.; Aoki, N.; Nakaishi, K.; Watabe, S.; Ito, E. Proposal of De Novo Antigen Test for COVID-19: Ultrasensitive Detection of Spike Proteins of SARS-CoV-2. *Diagnostics* **2020**, *10* (8), 594.
(40) Lassaunière, R.; Frische, A.; Harboe, Z.; Nielsen, A. C.; Fomsgaard, A.; Krogfelt, K.; Jørgensen, C. Evaluation of Nine Commercial SARS-CoV-2 Immunoassays. *medRxiv* **2020**, 1−15.
(41) Nash, B.; Badea, A.; Reddy, A.; Bosch, M.; Salcedo, N.; Gomez, A. R.; Versiani, A.; Celestino, D. S. G.; dos Santos, T. M. I. L.; Milhim, B. H. G. A.; Moraes, M. M.; Campos, G. R. F.; Quieroz, F.; Reis, A. F. N.; Nogueira, M. L.; Naumova, E. N.; Bosch, I.; Herrera, B. B. The Impact of High Frequency Rapid Viral Antigen Screening on COVID-19 Spread and Outcomes: A Validation and Modeling Study. *medRxiv* **2020**, 1−41.

https://dx.doi.org/10.1021/acscentsci.0c01309
ACS Cent. Sci. 2021, 7, 156−163